CACULATION OF BED VARIATION IN CURVED CHANNELS

TE-YUNG HSIEH [1] and JINN-CHUANG YANG [2]

[1] Researcher, Dept. of H100, EEL., Industrial Technology Research Institute
(Rm. 106, Bldg. 24, 195, Sec. 4, Chung Hsing Rd., Chutung, Hsinchu County 310, Taiwan, R.O.C.)
Phone +886 3 5918542/ Fax +886 3 5820017
E-mail: hsieh0182@itri.org.tw
[2] Professor, Dept. of Civil Eng., and Hazard Mitigation Research Center, National Chiao Tung Univ.,
(1001 Ta Hsueh Rd., Hsinchu 30050, Taiwan, R.O.C.)
Phone +886 3 5712121 ext 55268/ Fax +886 3 5918542
E-mail: jcyang@mail.nctu.edu.tw

An unsteady 2D depth-averaged mobile-bed model is developed and applied to compute the bed deformation in curved alluvial channels. The vertical velocity shape functions in the longitudinal and transverse directions proposed by de Vriend (1977) are adopted. The lateral dispersion coefficient for the channel bend is modeled by Fischer et al.'s (1979) formula. The bed-load transport direction angle by Struiksma et al. (1985) is used. Data from Struiksma's(1983) experiment are used to demonstrate the model's applicability for the bed deformation in curved channels. The calibration process by adjusting the parameters appearing in the function with one set of Struiksma's experiment and verified with the other set. The results show that the bed evolution phenomenon along the bend can be well modeled with suitable calibration of bed-load transport angle function.

Key Words : *two-dimensional models, depth averaged, mobile-bed, channel bends, secondary current*

1. INTRODUCTION

An understanding of flow and sediment transport in curved channels is important for hydraulic engineering. In curved channels, the secondary-current phenomenon is three- dimensional (3D) and many 3D numerical models have been developed to simulate the complicated problem. However, hydraulic engineers in practice often adopt 2D depth- averaged models because of their simplicity of implementation and application.

In the past decade, many researchers have developed several types of 2D depth-averaged model to study the bed deformation in curved channels. Engelund's (1974) model ignored the local derivative term and is applicable only for steady flow conditions. Struiksma et al. (1985) and Kassem and Chaudhry's (2002) models ignored the dispersion stress terms and the mechanism of suspended load and assumed the vertical flow velocity with uniform distribution. Struiksma et al. (1985) and Kassem and Chaudhry (2002) pointed out that the bed-load transport direction angle function should include the effects of channel slope, flow velocity, and channel curvature which in fact will be adopted in the model developed in this study. Engelund's (1974) model ignored the channel-slope and flow-velocity effects. Kikkawa et al. (1976) and Shimizu and Itakura (1989) ignored the channel-slope effect.

The purpose of this paper is to develop an unsteady 2D depth-averaged mobile-bed model for bed deformation in curved channels. In this model, the orthogonal curvilinear coordinate system is adopted and the suspended load and bed load are treated separately. Moreover, the secondary-current effect on water flow, suspended load and bed load equations are all embedded in the model. The implicit two-step split-operator approach (Hsieh and Yang 2004) is used to solve the flow governing equations; and the coupling approach with iterative method are

used to solve the mass-conservation equation of suspended sediment, mass- conservation equation of active-layer sediment, and global mass-conservation equation for bed sediment simultaneously. The experimental data measured by Struiksma (1983) are used to examine the capabilities of the proposed model in simulating the bed deformation in curved channels.

2. DESCRIPTION OF MODEL

(1) Governing Equations

a)Flow Equations

Continuity equation

$$h_1 h_2 \frac{\partial d}{\partial t} + \frac{\partial}{\partial \xi}(h_2 \bar{\bar{u}} d) + \frac{\partial}{\partial \eta}(h_1 \bar{\bar{v}} d) = 0 \qquad (1)$$

Momentum equations

$$\frac{\partial \bar{\bar{u}}}{\partial t} + \frac{\bar{\bar{u}}}{h_1}\frac{\partial \bar{\bar{u}}}{\partial \xi} + \frac{\bar{\bar{v}}}{h_2}\frac{\partial \bar{\bar{u}}}{\partial \eta} + \frac{1}{h_1 h_2}\frac{\partial h_1}{\partial \eta}\bar{\bar{u}}\bar{\bar{v}} - \frac{1}{h_1 h_2}\frac{\partial h_2}{\partial \xi}\bar{\bar{v}}^2 = -\frac{g}{h_1}\frac{\partial}{\partial \xi}(z_b + d) + \frac{1}{\rho h_1 h_2 d}\left[\frac{\partial}{\partial \xi}(h_2 T_{11}) + \frac{\partial}{\partial \eta}(h_1 T_{12}) + \frac{\partial h_1}{\partial \eta}T_{12} - \frac{\partial h_2}{\partial \xi}T_{22}\right] - \frac{\tau_{b_1}}{\rho d} + \frac{1}{\rho h_1 h_2 d}\left[-(h_2\tau_{11})_s\frac{\partial z_s}{\partial \xi} + (h_2\tau_{11})_b\frac{\partial z_b}{\partial \xi} - (h_1\tau_{12})_s\frac{\partial z_s}{\partial \eta} + (h_1\tau_{12})_b\frac{\partial z_b}{\partial \eta}\right] \qquad (2)$$

$$\frac{\partial \bar{\bar{v}}}{\partial t} + \frac{\bar{\bar{u}}}{h_1}\frac{\partial \bar{\bar{v}}}{\partial \xi} + \frac{\bar{\bar{v}}}{h_2}\frac{\partial \bar{\bar{v}}}{\partial \eta} + \frac{1}{h_1 h_2}\frac{\partial h_2}{\partial \xi}\bar{\bar{u}}\bar{\bar{v}} - \frac{1}{h_1 h_2}\frac{\partial h_1}{\partial \eta}\bar{\bar{u}}^2 = -\frac{g}{h_2}\frac{\partial}{\partial \eta}(z_b + d) + \frac{1}{\rho h_1 h_2 d}\left[\frac{\partial}{\partial \xi}(h_2 T_{12}) + \frac{\partial}{\partial \eta}(h_1 T_{22}) - \frac{\partial h_1}{\partial \eta}T_{11} + \frac{\partial h_2}{\partial \xi}T_{12}\right] - \frac{\tau_{b_2}}{\rho d} + \frac{1}{\rho h_1 h_2 d}\left[-(h_2\tau_{12})_s\frac{\partial z_s}{\partial \xi} + (h_2\tau_{12})_b\frac{\partial z_b}{\partial \xi} - (h_1\tau_{22})_s\frac{\partial z_s}{\partial \eta} + (h_1\tau_{22})_b\frac{\partial z_b}{\partial \eta}\right] \qquad (3)$$

in which ξ and η = orthogonal curvilinear coordinates in streamwise axis and transverse axis, respectively; h_1 and h_2 = metric coefficients in ξ- and η- directions, respectively; u and v = velocity components in ξ- and η- direction, respectively; ρ = fluid density; g = gravitational acceleration; t = the time; d = depth; z_b = bed elevation; z_s = water surface elevation; double overbar ($\bar{\bar{}}$) = depth average; subscripts s and b indicate the dependent variables at the water surface and channel bed, respectively; and T_{11}, T_{12}, T_{22} = effective stresses which consist of laminar viscous stresses, turbulent stresses and integrated dispersion stresses. The Boussinesq eddy-viscosity concept to simulate laminar viscous stresses and turbulent stresses, as described in details by Hsieh and Yang (2003). The treatment of dispersion stresses terms

$D_{11} = \int_{z_b}^{z_s}[-\rho(\bar{u} - \bar{\bar{u}})^2]dz$, $D_{22} = \int_{z_b}^{z_s}[-\rho(\bar{v} - \bar{\bar{v}})^2]dz$, $D_{12} = D_{21} = \int_{z_b}^{z_s}[-\rho(\bar{u} - \bar{\bar{u}})(\bar{v} - \bar{\bar{v}})]dz$ will be described in the following paragraph and overbar ($\bar{}$) denotes time average. $\tau_{b1} = C_f \rho \bar{\bar{u}}(\bar{\bar{u}}^2 + \bar{\bar{v}}^2)^{1/2}$ and $\tau_{b2} = C_f \rho \bar{\bar{v}}(\bar{\bar{u}}^2 + \bar{\bar{v}}^2)^{1/2}$ are the shear stresses at the channel bottom in the ξ- and η- directions, respectively; $C_f = g/c^2$ = friction factor; and c = Chezy factor.

b)Sediment Transport Equations

Mass-conservation equation of suspended sediment

$$\frac{\partial \bar{\bar{C}}}{\partial t} + \frac{\bar{\bar{u}}}{h_1}\frac{\partial \bar{\bar{C}}}{\partial \xi} + \frac{\bar{\bar{v}}}{h_2}\frac{\partial \bar{\bar{C}}}{\partial \eta} = -\frac{1}{h_1 h_2 d}\frac{\partial}{\partial \xi}(h_2 Q_1 d) - \frac{1}{h_1 h_2 d}\frac{\partial}{\partial \eta}(h_1 Q_2 d) + \frac{S}{\rho d} \qquad (4)$$

Mass-conservation equation of active-layer sediment

$$\rho_s(1-p)h_1 h_2 \frac{\partial(\beta E_m)}{\partial t} + \frac{\partial}{\partial \xi}(h_2 q_{b_1}) + \frac{\partial}{\partial \eta}(h_1 q_{b_2}) + S - S_f = 0 \qquad (5)$$

Global mass-conservation equation for bed sediment

$$\rho_s(1-p)h_1 h_2 \frac{\partial z_b}{\partial t} + \sum[\frac{\partial}{\partial \xi}(h_2 q_{b_1}) + \frac{\partial}{\partial \eta}(h_1 q_{b_2}) + S] = 0 \qquad (6)$$

where C = concentration; ρ_s = density of sediment; β = active-layer size fraction; p = porosity of the bed material; E_m = active-layer thickness (Spasojevic and Holly 1990); q_{b_1}, q_{b_2} = components of bedload flux in the ξ- and η- directions, respectively; S = suspended-sediment source; S_f = active-layer floor source (Spasojevic and Holly 1990); Q_1, Q_2 = suspended-sediment flux due to both turbulent diffusion and lateral dispersion in the ξ- and η- directions, respectively.

The bed-load flux adopted in this study is presented herein as:

$$q_{b_i} = \zeta \beta q_{b_i}^t \qquad (7)$$

where $q_{b_i}^t$ = theoretical bedload transport capacity in the i (ξ or η) direction, evaluated using Van Rijn's (1984a) formula. This load is adjusted by ζ, a so-called hiding factor. In this study, Karim el al.'s (1987) empirical relation is used to evaluate ζ. The adjusted load is modified by β to reflect the availability of the particular size-class in the active-layer elemental volume.

The suspended-sediment source S is the

combination of deposition and resuspension and can be expressed as

$$S = S_e - S_d \tag{8}$$

where $S_e = \rho w_l \beta C_e$ = entrainment component; $S_d = \rho w_f C_d$ = deposition component; w_l = lift-off velocity (Hu and Hui 1996); C_e = entrainment near-bed concentration (van Rijn's 1984b); w_f = sediment fall velocity (Van Rijn 1984b); C_d = near-bed deposition concentration (Lin 1984).

Q_1 and Q_2 appearing in Eq. (4) can be represented by a simple gradient transport model (Almquist and Holley 1985; Hsieh and Yang 2005)

$$Q_1 = \varepsilon_\xi \frac{\partial \overline{\overline{C}}}{\partial \xi} \quad ; \quad Q_2 = (\varepsilon_\eta + e_\eta)\frac{\partial \overline{\overline{C}}}{\partial \eta} \tag{11}$$

where ε_ξ and ε_η = turbulent diffusion coefficients in the ξ- and η- directions, respectively (Elder 1959); e_η = lateral dispersion coefficient will be described in the following paragraph.

In the present study, the model adopts the conventional sorting and armoring techniques which were proposed by Bennet and Nordin (1977). In the model the river bed can be divided into several layers, and bed composition counting is accomplished through the use of two or three armor layers depending on whether scouring or deposition occurs during the time step.

(2) Treatment of Secondary-Current Effect

Shape functions for the vertical velocity are embedded in the dispersion stress terms to exhibit the effect of the secondary current. The velocity profiles in the longitudinal and transverse directions proposed by de Vriend (1977) are adopted in the present model:

$$\overline{u} = \overline{\overline{u}}\left[1 + \frac{\sqrt{g}}{kc} + \frac{\sqrt{g}}{kc}\ln\zeta\right] = \overline{\overline{u}} f_m(\zeta) \tag{12}$$

$$\overline{v} = \overline{\overline{v}} f_m(\zeta) + \frac{\overline{\overline{u}} d}{k^2 r}\left[2F_1(\zeta) + \frac{\sqrt{g}}{kc}F_2(\zeta) - 2\left(1 - \frac{\sqrt{g}}{kc}\right) f_m(\zeta)\right] \tag{13}$$

where $F_1(\zeta) = \int_0^1 \frac{\ln\zeta}{\zeta - 1} d\zeta$; $F_2(\zeta) = \int_0^1 \frac{\ln^2\zeta}{\zeta - 1} d\zeta$; $\zeta = (z - z_b)/d$ = dimensionless distance from the bed; and r = radius of curvature.

The secondary-current effect will exert an influence on the lateral dispersion coefficient, e_η. In this study, the formula proposed by Fischer et al. (1979) is used, which was derived for flow in very wide channel:

$$\frac{e_\eta}{u_* d} = 25\left(\frac{\overline{\overline{u}} d}{u_* r}\right)^2 \tag{14}$$

To include the effect of secondary current in bed-load transport equations, the concept of direction angle function α of the bed-load transport from Struiksma et al. (1985) and Kassem and Chaudhry (2002) is adopted in the model.

$$\tan\alpha = \frac{\sin\delta - \frac{1}{f_s\theta}\frac{\partial z_b}{\partial \eta}}{\cos\delta - \frac{1}{f_s\theta}\frac{\partial z_b}{\partial \xi}} \tag{15}$$

where f_s = shape factor of the particles; $\theta = \frac{\overline{\overline{u}}^2 + \overline{\overline{v}}^2}{c^2(s-1)D_{50}}$ = Shields parameter.

The direction δ of the bed shear stress is defined as

$$\delta = \tan^{-1}\left(\frac{\overline{\overline{v}}}{\overline{\overline{u}}}\right) - \tan^{-1}\left(\frac{Ad}{r}\right) \tag{16}$$

where the term, $\tan^{-1}(Ad/r)$ = deviation of the bed shear stress due to the secondary-current effect; A = coefficient.

(3) Numerical Methodology

The implicit two-step split-operator approach proposed by Hsieh and Yang (2004) is used herein for flow computation. The first step (dispersion step) is to compute the provisional velocity in the momentum equation without considering the pressure gradient and bed friction. The second step (propagation step) is to correct the provisional velocity by considering the effect of the pressure gradient and bed friction.

Dispersion step includes convection and diffusion terms. In order to catch the flow direction, a simple Hybrid scheme is used for the convection terms. Diffusion terms are discretized using the concept of control volume. Coupling with the convection and diffusion terms, the ADI scheme is adopted to solve the discretization equations. Propagation step includes pressure, gravity, and bottom shear stresses terms, and none of velocity gradient appears in this step. Propagation step can be discretized into a simple algebraic equation while the unknown can be solved directly. Similar to diffusion terms, the continuity equation can be discretized by using the concept of control volume and solved by the ADI scheme. The detailed computation methodologies can be referred to Hsieh and Yang (2004).

The primary sediment variables are interrelated each other through the auxiliary relations. It is obvious that from the arguments mentioned above, a

coupling approach has to be used to solve the system equations of sediment. The mass-conservation equation of suspended sediment is split into two successive steps: advection step and diffusion step. The advection step contains advection and source terms. In order to obtain the better accuracy of solution for the advection part, a characteristics approach is used herein. The diffusion step contains diffusion terms which will be discretized by using the concept of control volume. Similarly, in sediment transport processes, Eqs. (5) and (6) are discretized by the control-volume concept.

(4) Boundary Conditions

Three types of boundary, namely, inlet, outlet and solid walls are considered. Discharge hydrograph per unit width, concentration distribution, bed elevation, and active-layer size fraction can be specified along the inlet section. Water surface elevation, $\partial\overline{\overline{C}}/\partial\xi = 0$, $\partial z_b/\partial\xi = 0$, and $\partial\beta/\partial\xi = 0$ can be specified along the outlet section. At the solid boundaries, the law of the wall is applied outside the viscous sublayer and transition layer. The wall shear stress is used as the wall boundary condition and is substituted into the momentum equation in the wall region to solve for the velocity component parallel to the wall. Besides, $\partial\overline{\overline{C}}/\partial\eta = 0$, $\partial z_b/\partial\eta = 0$, and $\partial\beta/\partial\eta = 0$ are specified in the solid wall.

3. DEMONSTRATION

(1) Model Calibration

To investigate the applicability of the numerical model presented herein, bed deformations results computed are compared with those observed by Struiksma (1983) and with the results computed by Struiksma et al. (1985) model.

The measurement was obtained at the Delft Hydraulics Laboratory (DHL) using a 140° bend with a centerline radius of curvature of 12 m connecting with straight section at upstream and downstream of the bend. The layout of the flume is shown in Fig. 1. The channel cross section was rectangular and the width was 1.5 m.

In the case of T2 from Struiksma's (1983) experiments, the flume initially had a flat bed in the lateral direction and had a slope of 2.03×10^{-3} in the longitudinal direction. The Chezy factor was 28.8 $m^{1/2}/s$. The clean water discharge and water depth specified at the upstream and downstream end of the channel were 0.062 m^3/s and 0.1 m respectively. The sediment particle for the bed material can be regarded as uniform since the standard deviation is low and the representative diameter was 0.45 mm. The duration of the flow was 400 min and was long enough to establish equilibrium bed topography.

A mesh of 121×37 and a time interval Δt = 1 sec were used in the simulation. The value of porosity p was 0.4. The coefficients f_s and A appearing in bed-load transport angle function were 2 and 0.91, respectively (Kassem and Chaudhry 2002). The upstream boundary condition was the inflow discharge per unit width. The measured water-surface elevation and the no-slip condition were used for the downstream end and the channel banks, respectively.

The computed and measured bed configurations along two longitudinal sections are illustrated in Fig. 2. Both computed bed profiles clearly show the presence of a point bar and a pool near the beginning of the bend. Although the computed results by the proposed and Struiksma et al. (1985) models and measured bed configurations are qualitatively in good agreement, the heights of point bar and pool computed by both models are generally underestimated. Struiksma et al. (1985) noted that the shortcoming of their model was due to the constant f_s and A for all computation domains adopted in the bed-load transport direction angle function. However, the bed material in case T2 is uniform, standing on the physical view point, it is not reasonable to calibrate f_s , which substantially represent the shape effect of the particle property. Hence, the present study suggests that A should be a major parameter being adjusted for modeling the bed deformation in case T2.

By using the various values of A in various regions described above, the computed and measured bed-level variations along two longitudinal sections are illustrated in Fig. 3. Fig. 3 shows that the computed results satisfactorily match with the measured results. It can be noted that a point bar is formed at the inner bank while a pool occurs at the outer bank.

(2) Model Verification

In order to verify the capability of the proposed model, the model has been applied to case T1 from Struiksma's (1983) experiments, which has been carried out with the same flume as case T2, using the same values of the calibrated parameters as those used to obtain the bed topography prediction for case T2 given in Fig. 3. For case T1, the clean water inflow discharge was 0.047 m^3/s, the water depth specified at the downstream end of the channel was 0.08 m, the slope in the longitudinal direction was 2.36×10^{-3}, and the Chezy factor was 28.4 $m^{1/2}/s$.

Fig. 4 compares the computed and measured bed

levels profiles along the inner and outer banks. A pronounced point bar and pool configuration are observed with the measured point bar height. The agreement between the measured and computed bed level for case T1 is not quite as good as for case T2 near the outer bank entrance, in which the computed bed profile shifts some distance upstream with respect to the measured profile and the computed length of the pool is smaller than the measured length. This discrepancy may be the inherent uncertainties existing for the different relative strength of secondary current, SI . Except the region having some deviation described above, model results agree consistently with measured data along the whole channel bend region as shown in Fig. 4.

4. CONCLUSION

An unsteady 2D depth-averaged mobile-bed model is developed and applied to compute the bed deformation in curved alluvial channels. By using the constant shape factor f_s and coefficient A which appear in bed-load transport direction angle function for the whole domain in case T2 of Struiksma's(1983) experiments, the overshoot phenomenon near the entrance of channel bend can not be well reproduced by the simulation. The analysis performed in this study shows that the coefficient A should be appropriately calibrated along the channel bend for the modeling. The verification carried out for the case of T1 from Struiksma's(1983) experiments shows convincing results.

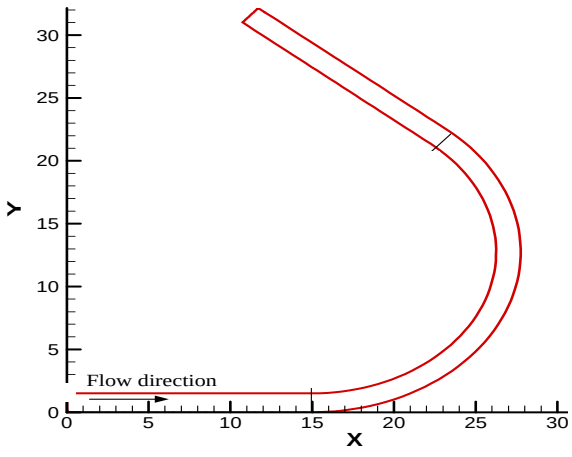

Figure.1 Channel geometry (Delft Hydraulics Laboratory flume)

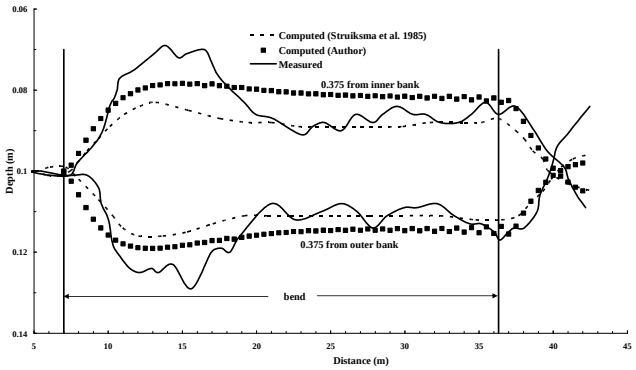

Figure.2 Prediction of longitudinal bed profiles using the constant coefficients in the case of T2 from Struiksma's (1983) experiments.

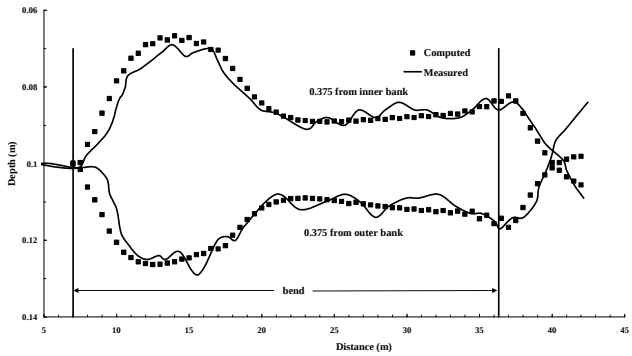

Figure.3 Prediction of longitudinal bed profiles using the non-constant coefficients A in case T2 of Struiksma's (1983) experiments.

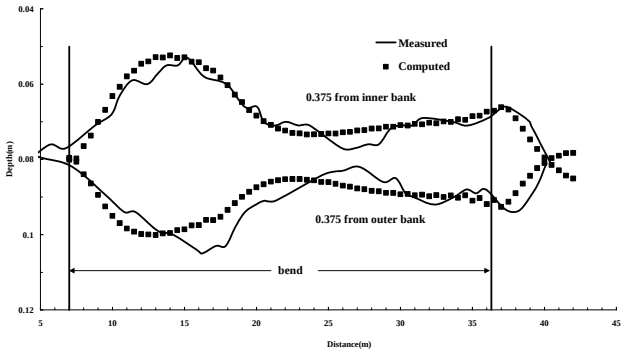

Figure.4 Prediction of longitudinal bed profiles using the non-constant coefficients A in case T1 of Struiksma's (1983) experiments.

REFERENCES

1) Almquist, C.W., and Holley, E.R. : Transverse mixing in meandering laboratory channels rectangular and naturally varying cross-section, *Tech. Rep. (205)*, Center for Research in Water Resources, University of Texas at Austin, 1985.
2) Bennett, J.P. and Nordin, C.F. : Simulation of sediment transport and armoring, Hydrological Sciences Bulletin, 37, 2119-2162, 1977.
3) de Vriend, H. J. : A mathematical model of steady flow in curved shallow channels, J. Hydr. Res., Delft, The Netherlands, 15(1), 37-54, 1877
4) Elder, J.W. : The dispersion of marked fluid in turbulent shear flow, J. Fluid Mech., Vol. 5, Part 4, 1979.
5) Engelund F. : Flow and bed topography in channel bends, J.

Hydr. Engrg., ASCE, 100(11), 1631- 1648, 1974.
6) Fischer, H.B., List, E.J, Koh, R.C.Y., Imberger, J., and Brookes, N.H. : Mixing in Inland and Coastal Waters, Academic, San Diego, 1979
7) Hsieh, T.Y., and Yang, J.C. : Investigation on the suitability of 2D depth-averaged models for bend-flow simulation, J. Hydr. Engrg., ASCE, 129(8), 597-612, 2003
8) Hsieh, T.Y. and Yang, J.C. : Implicit two-step split-operator approach for modelling two-dimensional open channel flow, Journal of Hydroscience and Hydraulic Engineering. 22, 2, 113-139, 2004.
9) Hsieh, T.Y. and Yang, J.C. : Numerical examination on the secondary-current effect for contaminant transport in crved channel, J. Hydr. Res., IAHR, 43(6), 643-658, 2005.
10) Hu, C., and Hui, Y. : Bed-load transport. I: Mechanical characteristics, J. Hydr. Engrg., ASCE, 122(5), 245-254, 1996.
11) Karim, M.F., Holly, F.M., and Yang, J.C. : IALLUVIAL: Numerical simulation of mobile-bed rivers: Part I, Theoretical and numerical principles, Report No. 309., Iowa Institute of Hydraulic Research, University of Iowa, Iowa City, Iowa, 1987.
12) Kassem A. A., and Chaudhry M. H. : Numerical modeling of bed evolution in channel bends, J. Hydr. Engrg., ASCE, 128(5), 507- 514, 2002.
13) Kikkawa, H., Ikeda S., and Kitagawa, A. : Flow and bed topography in curved open channels, J. Hydr. Div., ASCE, 102(9), 1327- 1342, 1976.
14) Lin, B. : Current study of unsteady transport of sediment in China, Proceedings of Japan-China Bi-Lateral Seminar on River Hydraulics and Engineering Experiences, Tokyo-Kyoto-Sapporo, 337-342, 1984.
15) Shimizu Y. and Itakura T. : Calculation of bed variation in alluvial channels, J. Hydr. Engrg., ASCE, 115(3), 367- 384, 1989.
16) Spasojevic, M. and Holly, F.M. : 2-D bed evolution in natural watercourses-new simulation approach, J. Waterw. Port Coast. Ocean Eng., ASCE, 116(4), 425-443, 1990.
17) Struiksma, N. : Results of movable bed experiments in the DHL curved flume, Report on Experimental Investigation, Two Rep. No.R657-XVIII/ M1771, Delft Hydraulics Laboratory, Delft, Netherlands, 1983.
18) Struiksma, N., Olesen K. W., Flokstra, C., and de Vriend, H. J. : Bed deformation in curved alluvial channels, J. Hydr. Res., 23(1),57 – 79, 1985.
19) Van Rijn, L.C. : Sediment Transports, Part I: Bed load transport, J. Hydr. Engrg., ASCE, 110(10), 1431-1456, 1984a.
20) Van Rijn, L.C. : Sediment Transports, Part II: Suspended load transport, J. Hydr. Engrg., ASCE, 110(11), 1613-1641, 1984b.